



Contents lists available at ScienceDirect

Journal of Hydrology

journal homepage: www.elsevier.com/locate/jhydrol

Can tree tilting be used for paleoflood discharge estimations?

J.A. Ballesteros-Cánovas^{a,b,*}, J.F. Márquez-Peñaranda^c, M. Sánchez-Silva^c, A. Díez-Herrero^d,
V. Ruiz-Villanueva^a, J.M. Bodoque^e, M.A. Eguibar^f, M. Stoffel^{a,b}

^a Dendrolab.ch, Institute of Geological Sciences, University of Bern, Baltzerstrasse 1+3, 3012 Bern, Switzerland

^b Institute for Environmental Sciences, University of Geneva, 7 route de Drize, 1227 Carouge, Geneva, Switzerland

^c Department of Civil and Environmental Engineering, Universidad de Los Andes, Bogotá, Colombia

^d Department of Research and Geoscientific Prospective, Geological Survey of Spain (IGME), Ríos Rosas 23, Madrid E-28003, Spain

^e Mining and Geological Engineering Department, University of Castilla-La Mancha, Campus Fábrica de Armas, Avda. Carlos III, Toledo E-45071, Spain

^f Institute for Water and Environmental Engineering (IIAMA), Technical University of Valencia, Department of Hydraulic Engineering and Environment, Valencia, Spain

ARTICLE INFO

Article history:

Available online xxxxx

Keywords:

Paleohydrology

Tree rings

Tilted trees

Flood

Peak discharge

SUMMARY

Paleoflood hydrology typically deals with the reconstruction of floods in ungauged and poorly gauged basins by combining different sources of indirect evidence. Botanical indicators have been used repeatedly in the past, mostly through the study of scars in trees or germination dates of plants on newly created surfaces. In this paper we test the hypothesis that the inclination of trees – as induced by floods – can provide information on flood magnitude, and that this source of information can therefore be used for flood reconstructions. We used a mechanical root-plate rotational stiffness model in three gauged river reaches in Central Spain to test our hypothesis and combine approaches typically applied in dendrogeomorphic, dendrometric, mechanical structure, and hydraulic research. Results show a correlation between modeled and observed deformation at the stem base of trees induced by floods (coefficient of correlation 0.58 for all observations). However they also point to a clear underestimation of peak discharge reconstructions. We used different efficiency criteria to test the reliability of results and differences between river reaches. In addition, we carried out a sensitivity analysis and discussed sources of uncertainties which may reach up to 112%, mainly due to difficulties to determine the rotational stiffness of the root plate system a posteriori. The approach presented here is promising, but more research is clearly required to improve the quality of peak discharge estimations based on stem tilting.

© 2014 Elsevier B.V. All rights reserved.

1. Introduction

The scarcity of instrumental data and the shortness of records severely hamper the acquisition and development of reliable and representative flood time series and add considerable uncertainty to flood hazard assessment (Brázdil et al., 2006). This lack of data also largely hinders the analysis of flood magnitude and frequency and calls for the application of alternative and/or complementary approaches. Paleoflood hydrology deals with the reconstruction of the magnitude and frequency of recent, past, or ancient ungauged floods by combining indirect evidence, hydraulic methods and statistical techniques (Baker et al., 2002; Benito et al., 2003). Over the last 30 years, paleoflood hydrology has achieved

recognition as a new branch of geomorphology and hydrology (Baker et al., 2002; Benito and Thorndyraft, 2005; Baker, 2008) by employing geologic, hydrologic, and fluid dynamic principles to infer quantitative as well as qualitative aspects of unrecorded floods (House et al., 2002). Therefore, it has been recognized that the use of paleohydrologic techniques provides one means of evaluating the hydrologic effects of long-term hydrologic variability and climatic change at ungauged locations, and is useful to decrease uncertainty in hydrologic estimations (Jarrett, 1991).

Botanical evidence represents an indirect indicator of past flood events (Sigafos, 1964; Baker, 2008). Botanical evidence can be interpreted by means of dendrogeomorphic approaches (Stoffel et al., 2010; Stoffel and Corona, 2014; Ballesteros-Cánovas et al., in preparation) and has been demonstrated to be a very reliable tool for the spatio-temporal reconstruction of past floods in mountain environments (Ballesteros et al., 2010; Ballesteros-Cánovas et al., 2011a,b; Arbellay et al., 2012). Among all existing botanical flood evidence, scars (injuries) on stem have been used most extensively because of their ability to provide information about the

* Corresponding author.

E-mail addresses: juan.ballesteros@dendrolab.ch (J.A. Ballesteros-Cánovas), jf.marquez53@uniandes.edu.co (J.F. Márquez-Peñaranda), msanchez@uniandes.edu.co (M. Sánchez-Silva), andres.diez@igme.es (A. Díez-Herrero), virgina.ruiz@dendrolab.ch (V. Ruiz-Villanueva), josemaria.bodoque@uclm.es (J.M. Bodoque), mequibar@hma.upv.es (M.A. Eguibar), markus.stoffel@dendrolab.ch (M. Stoffel).

<http://dx.doi.org/10.1016/j.jhydrol.2014.10.026>

0022-1694/© 2014 Elsevier B.V. All rights reserved.

Nomenclature

<i>ac</i>	aplication center of the drag force (m)	M_{base}	bending moment acting at the stem base (Nm)
<i>Arw</i>	<i>unidimensional</i> parameter comparing the proportions of the root-soil plate weight of the total below-ground anchorage (Coutts, 1983)	M_{res}	maximum (resistant) stem base bending moment (Nm)
<i>cgc</i>	crown centroid (m)	<i>mwd</i>	floating wood mass (kg)
<i>cgt</i>	tree centroid (m)	<i>RPD</i>	root plate depth (m)
<i>cgs</i>	stem centroid (m)	<i>RPL</i>	root plate length (m)
<i>DBH</i>	diameter at breast height (m)	<i>RPW</i>	root plate width (m)
D_c	drag coefficient (dimensionless)	<i>S</i>	tree surface exposed to flow (m ²)
<i>Fd</i>	drag force (N)	<i>V</i>	flow velocity (m s ⁻¹)
F_{wd}	equivalent force generated by the woody material (N)	<i>W</i>	tree weight (N)
<i>g</i>	gravity (m s ⁻²)	W_D	water depth (m)
<i>hc</i>	crown height (m)	W_c	crown weight (N)
<i>hs</i>	stem height (m)	W_s	stem weight (N)
<i>ht</i>	height of tree (m)	ρ_s	bulk soil density (kg m ⁻³)
<i>hw</i>	thickness of woody debris (m)	ρ_w	wood density (kg m ⁻³)
k_i	rotational stiffness of the root plate system (Nm/rad)	ρ_c	crown density (kg m ⁻³)
K_m	maximum rotational stiffness of the root plate system (Nm/rad)	θ	deformation at the base of the tree (rad)
		θ_i	initial deformation (residual) at the base of the tree (rad)
		θ_e	elastic limit deformation at the base of the tree (rad)

timing and the level reached during a flood (Gottesfeld, 1996; Yanosky and Jarrett, 2002; St. George, 2010; Ruiz-Villanueva et al., 2010; Ballesteros-Cánovas et al., 2011b). Other botanical evidence is tilted trees. This evidence is due to a structural deformation of a tree resulting from unidirectional, hydrodynamic pressure on the stem during floods. Stem tilting will be accompanied by the formation of reaction wood in the tree-ring record, which can be used to date past geomorphic events (Stoffel et al., 2010).

On the other hand, structural analysis of trees under external loads has been studied over the last decade as well, but with a focus on root-soil interactions. Field experiments have been used to show the role of roots and soil tension and root plate size in root-plate anchorage of trees under external loads (Coutts, 1983; Stokes, 1999; England et al., 2000; Dupuy et al., 2005, 2007; Fourcaud et al., 2008). In addition, various engineering approaches – including Euler–Bernoulli beams analysis – have been proposed to describe elastic deflection and ultimate resistance of trees (Neild and Wood, 1999). Most efforts have been focused on wind force as the main external load (Gardiner et al., 2000; Watson, 2000; Ancelin et al., 2004; Danjon et al., 2005; Peltola, 2006; Coder, 2010), whereas impacts of other external loads such as snow accretion (Kato and Nakatani, 2000), typhoons (Chiba, 2000), or rockfalls (Stokes et al., 2005) have been less profusely analyzed. In the same line of thinking, it seems appropriate to think that tilted trees growing in floodplains may exhibit reactions induced by flood, and that their structural behavior could be linked to flow conditions and ultimately flood magnitude.

In this paper, we will therefore explore the utility of tilted trees for peak discharge estimation of paleofloods through the application of a mechanical model to reproduce the base deformation of trees under hydrodynamic forces during floods. We compare results with deformation values observed in the stem base of 35 trees (i.e. *Alnus glutinosa*, *Fraxinus angustifolia*, and *Pinus sylvestris*) tilted by floods. Our paper represents a multi-disciplinary approach and combines dendrogeomorphic, dendrometric, structural mechanics and paleohydrologic techniques to determine if, based on our observations, it is possible to estimate peak discharge of past floods using stem tilting in trees.

2. Material and methods

2.1. Conceptual model of tree-deformation

Trees exposed to hydrodynamic forces will deflect in natural environments. For this reason, we use a conceptual approach where the rotational stiffness of the root-plate system represents the response to the moment generated by the hydrodynamic force and tree weight (Fig. 1).

In this approach, the rotation of the root-plate soil θ_i is considered equal to that of the stem base, so that the value of θ_i can be approximated following Jonsson et al., (2006, Eq. (1)):

$$\theta = \theta_i + \frac{M_{base}}{k_i} \quad (1)$$

where θ_i (rad) is the initial rotation of the root-soil plate, which was assessed null for the purpose of this study; k_i (Nm/rad) the rotational stiffness of the root plate; M_{base} (Nm, Eq. (2)) the stem base bending moment related to the demanding forces, i.e. the drag force (F_d , N, Eq. (3) and F_{wd} , N), tree weight ($W = W_s + W_c$, N, Eqs. (4) and (5)) and the force induced by wood deposited against the stem (F_{wd} , N, Eq. (4)). The lever arm of each force (measured from the stem base) is obtained by considering the real moment arm. Details on the application points and corresponding abbreviations are given in Fig. 1 and will be described in the following:

$$M_{base} = (F_d \times ac \times \cos \theta) + (W \times cgt \times \sin \theta) + (F_{wd} \times W_D) \quad (2)$$

The point *ac* is located at 50% of water depth, whereas *cgs*, *cgc*, *cgt* represent the position of the stem, crown and tree centroids, respectively, W_D is the total water depth.

The drag force F_d in Eq. (3) is associated with (i) water density (ρ), (ii) drag coefficient (D_c), (iii) tree surface exposed to the flow (S , m²); and (iv) flow velocity (\bar{V} , m s⁻¹). Water density was assessed as ~ 1000 kgf m⁻³. The expected initial drag coefficient D_c is considered to be equal to 1 based on Bruschi et al. (2003). D_c is a dimensionless measurement used to represent the resistance imposed against flow by an object within a fluid environment, it can decrease exponentially with flow velocity (Vogel, 1989).

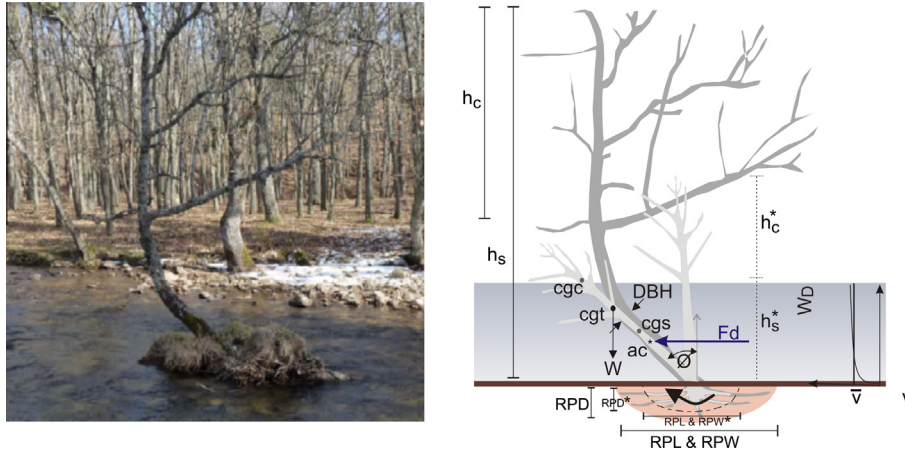


Fig. 1. Scheme of forces of hydrodynamic loads acting on a tree during flood causing it to tilt, where *cgc* is the crown centroid; *cgt* the tree centroid; *cgs* the stem centroid; *W* the tree weight; *DBH* the tree diameter at breast height; *Fd* the drag force; *Fwd* the equivalent force generated by the woody material; *ac* the application center of this equivalent force; *hs* and *hc* are the total height and the height of the treetop of the actual tree; *hs** and *hc** are the same heights of the young tree when it was tilting; ϕ the final rotation of the tree; *RPD*, *RPL* and *RPW* are the root plate depth, length and width respectively; *V* the average flow velocity, and *Wd* the water depth.

In Eqs. (4) and (5), h_t is tree height, *DBH* is tree diameter at breast height, ρ_w is wood density (defined as 8.0 KN m^{-3} and 4.2 KN m^{-3} for broadleaved and conifer species, respectively), $w_c = 0.75h_t$ is crown width, and $\rho_c = 0.05\rho_w$ is crown density. Note that – in line with Ancelin et al. (2004) – h_s (m) and w_c (m) are defined here as functions of h_t .

$$F_d = 0.5 \times \rho \times D_c \times S \times V^2 \quad (3)$$

$$W_s = \frac{0.4h_t \times \pi \times DBH^2}{4} \times \rho_w \times g \quad (4)$$

$$W_c = \frac{0.6h_t \times \pi \times w_c \times \rho_c \times G}{8} \quad (5)$$

The equivalent force F_{wd} (N) generated by woody debris is calculated via the kinetic energy related to a floating woody mass *mwd* (kgf) transported at a velocity equal to that of the water flow as measured at the surface *V* (m s^{-1}). This kinetic energy is converted to strain energy in the tree body and is related to an equivalent force capable to move the tree horizontally and at an amount equal to $hw \times \sin \theta$ (m). Therefore the value of the equivalent force of the impact of floating woody material on trees can be calculated as (Eq. (6)):

$$F_{wd} = \frac{mwd \times \bar{V}^2}{2 \times hw \times \sin \theta} \quad (6)$$

The maximum root-plate rotational stiffness K_m has been addressed by means of the ratio between the expected maximum resistive moment (M_{res}) and the expected elastic angle of the root plate (θ_e) by using Eq. (7):

$$k_m = \frac{M_{res}}{\theta_e} \quad (7)$$

where M_{res} (Nm, Eq. (8)) is estimated as a function of the root-plate size and soil properties according to the equation proposed by Peltola (1990):

$$M_{res} = \frac{g \times RPM \times RPD}{Arw} \quad (8)$$

where *RPM* (details provided in Eq. (9)) and *RPD* represent the mass and depth of the root plate and where *Arw* indicates the ratio between total stem-root system resistance and root-plate weight. In this study, we assessed *Arw* through a relative comparison

between the proportions of the root-soil plate weight of the total below-ground anchorage (Coutts, 1983).

$$RPM = \frac{(\pi \times RPL \times RPW \times RPD)}{3} \times \rho_s \quad (9)$$

where *RPL*, *RPW*, and *RPD* (m) are the length, width and depth of the root-plate respectively, and ρ_s is the soil density.

2.2. Model parameterization

2.2.1. Field data acquisition

The model parameterization was performed in three river reaches in Central Spain. The Tagus River is the longest river of the Iberian Peninsula. The total area to the gauging station in Peralejos de las Truchas is 410 km^2 , and altitudes range between 1920 and 1143 m a.s.l. The Alberche River is a right margin tributary of the Tagus River. The basin area at Navaluenga is 698 km^2 , and altitudes range from 2293 to 753 m a.s.l. The Cega River is a left tributary of the Duero River. The total basin area at the gauging station in Pajares de Pedraza is 280 km^2 , and altitudes range between 2209 and 938 m a.s.l.

The flora of the river basins is composed of Mediterranean forests (*Quercus* sp. and *Juniperus* sp.) with some Eurosiberian influence (mainly *Pinus pinaster* and *P. sylvestris*). The riverine formations are formed by willow-alder forests with *Salix* sp. and *Populus* sp., plus *F. angustifolia* in the case of the Alberche and Cega Rivers. The geomorphic configuration in the Alberche and Cega Rivers results from the Alpine orogeny (Miocene) which formed push-up mountain blocks and push-down basins overlain by Quaternary slope cover of glacial and periglacial origin. In the case of the Tagus River study site, Alpine orogeny (Cenozoic) resulted in a mountain system with several fold-and-thrust belts. The incision of the drainage network has formed deep canyons and gorges in these structural reliefs.

In these reaches gauge stations exist next to the sampling sites (<100 m), where different tree species (*A. glutinosa*, *F. angustifolia* and *P. sylvestris*) growing next to the river beds exhibit tilted stems (Fig. 2). All tilted trees were located in the field with a GPS (accuracy < 3 m) and sampled with an increment borer so as to date the initiation of reaction wood (Stoffel et al., 2010; Stoffel and Corona, 2014). Only trees (i) showing a deformation at the stem base, (ii) being exposed to flood flows and (iii) lacking scars on the stem surface were considered for analysis so as to avoid consideration of energies induced by punctual impacts. The sampling procedure

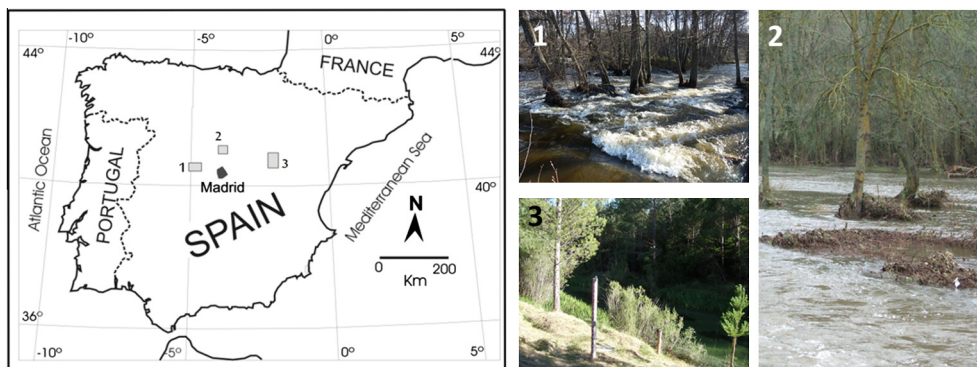


Fig. 2. Location of the river reaches investigated: (1) Alberche, (2) Cega, and (3) Tagus rivers.

in the field consisted in the extraction of two increment cores at the point of maximum curvature of the stem in the direction of the tilting.

Then we measured the tree height, stem height and DBH of undisturbed neighboring trees to determine the relation between DBH and H_t . By using the distance between the pith and the location where reaction wood starts to occur on the tree's cross-section, we used the relation between DBH and H_t to estimate tree size at the moment of flood occurrence (=moment of tilting). General dendrometric relations based on solid of revolution were used to obtain the tree and stem height at the moment of tilting as follows: $\frac{DBH}{2} = p \times \sqrt{H_t^n}$, where the type was fitted with a neiloide in case that $n = 3$, and with a paraboloid in case $n = 1$ (Husch et al., 1982). Wood deposit sizes were then characterized (i.e. length and width) based on the deposits found around trees. As wood deposits may vary depending on channel elevation (Pettit et al., 2005; Mikuš et al., 2013), measurements were undertaken in the floodplain and at the same channel level. Roughness was determined based on land use according to Chow (1959) and Lidar data (DEM 1×1 m) and cross profiles were used as topographic data. In a final step, soils were characterized with short vertical profiles of small trenches (100 cm long, 20 cm wide, 30–40 cm deep). In addition, we visually classified soil units according to the USDA soil taxonomy (USDA, 1999).

2.2.2. Dendrogeomorphic analysis of tilted trees and their relation with flood events

Samples were prepared following the methods described in Stoffel and Corona (2014), scanned at 2400 dpi and tree rings measured with WinDendro software. Reaction wood was detected in the tree-ring records via (i) abrupt changes in ring widths and (ii) microscopic changes in tree cell form and sizes (Timell, 1986; Braam et al., 1987; Lopez-Saez et al., 2012).

Based on the analysis of flow series from the river gauge station, the occurrence of reaction wood was assigned to peak flows recorded in the same year. In this step, only years with significant flood occurrences were considered. In addition, based on the rating curve, we obtained water depths for each flood event. To take account of possible changes in channel topography or malfunction of the gauge station we only took account of years where the rating curve showed a stable behavior.

2.2.3. Root plate anchorage

The anchoring of the soil–root system is the main mechanism to resist uprooting stress generated in trees by weight and hydrodynamic loads. In this study, we used approaches based on root-plate size characteristic as indirect indicators of maximum root-plate anchorage (Peltola, 2006). Root-plate size models were obtained

from a 3D inspection of affected in *A. glutinosa* and *F. angustifolia* with a multi-frequency georadar (GPR) inspection (Ballesteros et al., in preparation), whereas bibliographic sources were used to assess M_{res} in *P. sylvestris* (Stokes, 1999; Lundström et al., 2007; Nicoll et al., 2008; Bergeron et al., 2009). For the computation of rotational stiffness, maximum resistive moment was set at an elastic angle of the root-plate close to $15 \pm 10^\circ$ (Coutts, 1983; Cucchi and Bert, 2003; Jonsson et al., 2006; Lundström et al., 2007).

2.2.4. Hydraulic models and drag coefficient

The hydrodynamic model IBER (<http://www.iberaula.es>) were used to obtain water depth and flow velocities. IBER simulates turbulent free surface unsteady flows and environmental processes in river hydraulics and solves depth averaged two-dimensional shallow water (2D Saint-Venant) equations using finite volume methods with a second-order roe scheme. This method is particularly suitable for flows in mountain rivers where shocks and discontinuities can occur and flow hydrographs tend to be very sharp. The method is conservative, even in case that wetting and drying processes occur. The model works in a non-structured mesh consisting of triangle or quadrilateral elements. Inlet water discharge was computed using peak discharge (steady flow) from the stream gauge records. Bed friction is evaluated using Manning's n roughness coefficient, which was initially assessed using homogenous roughness units (Chow, 1959) and later calibrated with rating curves from real gauge stations.

2.3. Model efficiency and sensitivity analysis

Three different criteria have been used to determine the efficiency of results, namely the Nash–Sutcliffe efficiency index (NS, Nash and Sutcliffe, 1970), the coefficient of determination

Table 1

Parameters, units and value changes used in the sensitivity analysis, where H_t^* is tree height (m); V is flow velocity (m s^{-1}); W_D is water depth (m); D_c gives the drag coefficient (dimensionless); M_{res} is the resistive momentum; θ_e the elastic limit deformation at the tree base (rad), and where VS is the value changes used in the sensitivity analysis.

Parameter	Units	VS (%)
H_t^*	%	20
V	%	20
W_D	cm	20
Wood jam	%	20
D_c	%	20
Root-plate size	%	20
M_{res}	%	20
θ_e	rad	20

(Pearson), and the coefficient of correlation. The first two indices provide an idea about how consistent model results are, whereas the coefficient of correlation provides insights on the dependence of results with observed values. A sensitivity analysis was then carried out to define the impact on results as consequence to perform a variation of internal parameters by 20% (Table 1). A Principal Component Analysis (PCA) was then carried out to identify how variables affect outcomes of independent model variables.

3. Results

3.1. Available data

A total of thirty-five tilted trees were found and analyzed close to the gauge station in the study reaches, 16 *A. glutinosa* from the Alberche, 6 *F. angustifolia* from the Cega, and 13 *P. sylvestris* from the Tagus rivers. The analysis of reaction wood in increment cores has allowed determination of the bending moment of tree tilting. The average DBH at the time of tilting was 8.6 ± 5 cm in *A. glutinosa*, 9.1 ± 5.1 cm in *F. angustifolia*, and 16.6 ± 5.6 cm in *P. sylvestris*. Table 2 shows correspondences between the moment of tilting and the first major flood recorded by the flow gauge stations.

A total of 65 undisturbed, neighboring trees were measured in the floodplains to determine relationship between h_t and DBH. Table 3 shows relations between h_t and DBH as well as correlation coefficients for each species and each site. Variation between the estimated tree height h_t^* based on the relation between h_t and DBH and the internal diameter of trees at the moment of tilting

Table 3
Dendrometric models derived for each tree species.

River	Species	N°	Model	R ²
Alberche	<i>A. glutinosa</i>	25	$(\frac{DBH}{2})^2 = 7.57E - 04 \times (h_t^*)^3$	0.58
Cega	<i>F. angustifolia</i>	20	$(\frac{DBH}{2})^2 = 8.89E - 08 \times (h_t^*)^3$	0.81
Tagus	<i>P. sylvestris</i>	30	$(\frac{DBH}{2})^2 = 2.91E - 09 \times h_t^*$	0.85

was in the order of 2–6 m for *A. glutinosa*, 2–5 m for *F. angustifolia*, and 5–12 m for *P. sylvestris*. All trees investigated in this study were relatively young when tilted (for details see H_t and θ column 2 and 3, respectively, in Table 2).

Table 2 also provides information on the root-plate volume as obtained with GPR imagery in the case of *A. glutinosa* (Alberche River) and *F. angustifolia* (Cega River) and bibliography review in the case of *P. sylvestris* (Tagus River). The root-plate shape in both cases was associated with an ellipsoidal, with its long axis in the range of 0.4–1.46 m in *A. glutinosa* and 0.36–1.21 m in *F. angustifolia*, and a maximum root depth of 0.3 ± 0.15 and 0.26 ± 0.12 m, respectively. These empirical models were then used for the determination of root-plate volumes (which, in turn, ranged between 0.05 and 1.06 m³) and their maximum resistive moment, and consequently, their expected rotational stiffness (see Table 2).

Average flow velocities of past flood events were obtained through hydraulic modeling (Table 2), which, in addition, also allowed determination of water depths during past floods at the location of each tilted tree. Based on field measurement, Fig. 3

Table 2

Tree parameters used in this study. For details see text. ALB = Alberche (*Alnus glutinosa*), PAJ = Cega (*Fraxinus angustifolia*) and TAJ = Tagus (*Pinus sylvestris*) river. Flow velocity in the Cega River was estimated with 1D hydraulic model, whereas in Alberche and Tagus the flow velocity was estimated with 2D hydraulic models. (Abbreviations used: H_t = tree height; DBH = diameter of the tree at 1.30 m; Q = water flow; V = flow velocity; F_{wd} = force induced by wood deposited against the stem; θ = inclination at stem base; RPV = root plate volume; K = rotational stiffness; hg = height of center of gravity; ha = height of center of application, and M = the moment applied at the tree base by external forces, i.e. hydrodynamics forces and weight of the tree).

	H_t (m)	DBH (m)	Q (m ³ /s)	V (m/s)	F_{wd} (N)	θ (rad)	RPV (m ³)	K (N-m/rad)	hg (m)	ha (m)	M (N-m)
ALB01	3.00	0.07	487.00	1.60	14.12	0.90	0.10	2103	1.61	1.22	1374
ALB 02	3.00	0.08	487.00	1.59	9.50	0.41	0.12	2883	1.61	1.21	620
ALB 03	3.00	0.08	532.00	1.58	8.57	0.31	0.12	3243	1.61	1.26	504
ALB 04	2.50	0.05	532.00	1.40	7.43	0.43	0.06	1455	1.35	1.15	396
ALB 05	2.50	0.05	532.00	1.50	7.81	0.26	0.06	1636	1.35	1.17	284
ALB 06	3.00	0.07	532.00	1.50	10.09	0.66	0.10	2213	1.61	1.20	862
ALB 07	2.00	0.04	532.00	1.50	7.77	0.24	0.05	1349	1.08	1.06	179
ALB 08	2.50	0.05	532.00	1.50	8.37	0.31	0.06	1636	1.35	1.13	310
ALB 09	3.50	0.12	1168.00	2.05	9.82	0.47	0.24	5883	1.85	1.75	3190
ALB 10	5.00	0.18	1168.00	3.10	32.30	1.06	0.50	12106	2.64	2.32	35984
ALB 11	4.00	0.15	1168.00	3.60	29.23	0.76	0.35	8230	2.11	2.09	24449
ALB 12	3.00	0.07	532.00	1.50	9.21	0.61	0.10	2336	1.61	1.24	872
ALB 13	2.00	0.03	532.00	1.50	8.86	0.55	0.04	844	1.09	1.06	402
ALB 14	6.00	0.20	227.00	1.20	7.49	0.34	0.62	19112	3.18	0.65	735
ALB 15	2.50	0.05	532.00	1.50	8.65	0.40	0.06	1455	1.35	1.13	402
ALB 16	3.00	0.10	792.00	3.20	24.86	0.56	0.17	4209	1.59	1.58	6290
CEG01	5.00	0.16	73.00	1.48	61.53	0.54	0.40	10455	2.66	1.27	1471
CEG 02	4.00	0.06	42.00	1.22	74.44	0.87	0.08	1861	2.18	1.03	888
CEG 03	2.00	0.02	19.00	0.80	26.30	0.08	0.03	1374	1.09	0.72	7
CEG 04	4.00	0.08	67.00	1.10	29.06	0.29	0.12	3243	2.16	1.31	305
CEG 05	4.00	0.08	67.00	1.10	31.39	0.48	0.12	2883	2.16	1.31	578
CEG 06	5.00	0.14	26.00	0.80	26.06	0.55	0.31	7949	2.67	0.59	796
TAJ01	6.00	0.16	51.10	0.90	21.25	0.70	0.40	9410	3.21	1.46	1667
TAJ 02	10.00	0.22	38.04	0.70	29.11	0.87	0.75	19011	5.39	0.50	13830
TAJ 03	10.00	0.20	77.89	0.80	14.28	0.31	0.62	15290	5.40	0.90	1861
TAJ 04	6.00	0.16	159.20	1.00	20.81	0.26	0.40	11070	3.21	1.46	375
TAJ 05	5.00	0.10	159.20	1.20	21.90	0.26	0.17	4457	2.70	1.82	756
TAJ 06	6.00	0.18	94.39	1.30	45.68	0.49	0.50	12743	3.20	1.07	914
TAJ 07	6.00	0.14	94.39	1.30	45.17	0.52	0.31	7531	3.23	1.21	969
TAJ 08	10.00	0.22	38.04	1.00	56.75	0.28	0.75	22366	5.39	0.35	1513
TAJ 09	6.00	0.16	77.89	0.80	8.18	0.09	0.40	18820	3.21	2.09	180
TAJ 10	12.00	0.26	94.39	0.40	8.79	0.12	1.06	56590	6.47	0.35	594
TAJ 11	6.00	0.10	92.83	1.00	34.95	0.87	0.17	3788	3.26	1.35	1936
TAJ 12	5.00	0.06	30.73	0.80	81.47	1.05	0.08	1675	2.73	0.30	1076
TAJ 13	10.00	0.20	92.83	0.60	8.36	0.52	0.62	16095	5.40	0.95	5026

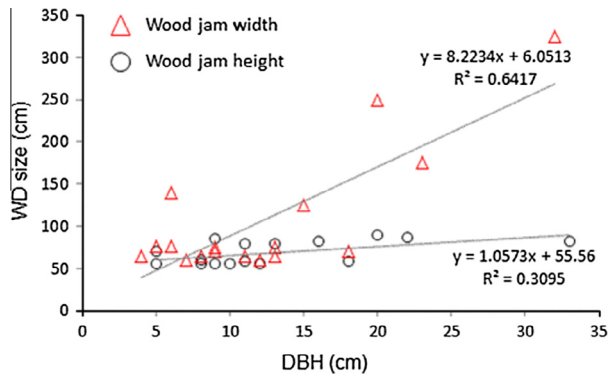


Fig. 3. Deposition of wood around stems (WD) as a function of tree diameter at breast height (DBH). Data are from Alberche River.

shows the general characterization of wood jams as found in the floodplains of the Alberche River. These wood jams increase the drag force, and were thus investigated in terms of their relationship with tree diameter. The computed force derived from wooden deposits is shown in Table 2 as well. Finally, Table 2 also provides information on the expected moment induced by hydrodynamic forces at the stem base, the weight and wood deposits.

3.2. Observed vs. modeled tree deformation during floods

Differences between observed and modeled deformation of trees are illustrated in Fig. 4, presented for each of the rivers, as well as for the three different efficiency criteria computed to determine the reliability of results. In comparison with observations models tend to underestimate results almost systematically. After removal of three outliers observed in the Alberche River, underestimation was in the order of 32–60%. The efficiency NS index for Cega and Tagus River was almost zero (−0.79 and 0.003, respectively), whereas in the case of the Alberche River and for the full dataset, the efficiency NS index was significantly smaller than zero with −10.9 and −4, respectively. Pearson and correlation

coefficients were 0.56 and 0.74, respectively, for Alberche River; 0.78 and 0.88 for Cega and Tagus rivers; whereas taking into account the full dataset of observations, the Pearson and correlation coefficients were significantly lower with 0.34 and 0.58.

The model results have to be seen in view of the various sources of uncertainties (Table 4) identified along the procedure, their origin and changes. Among these the dendrometric model can be seen as the most relevant source of uncertainty, as it directly conditions the root-plate size, along with the uncertainty related to θ_e . These sources of uncertainties may influence results by up to 112%.

3.3. Control parameters and analysis of sensitivity

The PCA carried out to explain the contribution of the main variables describing tree characteristics (zone, DBH and H_t), observed deformation and hydraulic condition (\bar{V}) on the discrepancy of the model (O/M i.e. differences between observed and modeled) shows that in fact two factors explain most (80.3%) of the variability (Fig. 4). The first factor (51.8%) is related the tree characteristics with correlations of 0.86, 0.83 and 0.65 for zone, H_t , and DBH , respectively; whereas the second factor (28.5%) is related to \bar{V} and O/M, with correlations of −0.83 and −0.67, respectively. The Pearson coefficient between \bar{V} and O/M (0.9) indicates that the model does not yield good data in the case of large floods characterized by high flow velocities. This observation is well in concert with the flood characteristics (velocities $> 3.1 \text{ m s}^{-1}$) as observed during the event which caused the tree outliers in the trees sampled at Alberche River (Fig. 5).

The PCA analysis given in Fig. 5 shows that the main sources of uncertainties are associated with variables related to tree size and flood flow conditions. If compared with the results of the sensitivity analysis of changes in internal model parameters (Table 1), we realize that the variables included as first and second factors in the PCA are virtually congruent between the two approaches. We state that major changes in model output are related with changes in variables depending on tree size. For instance, a 20% change in H_t and root-plate size parameters will result in values of tree deformation differing by 46.9% and 52%, respectively. However, variations in variables related to flow conditions showed similar changes in results as well. A change of water depths by 20%

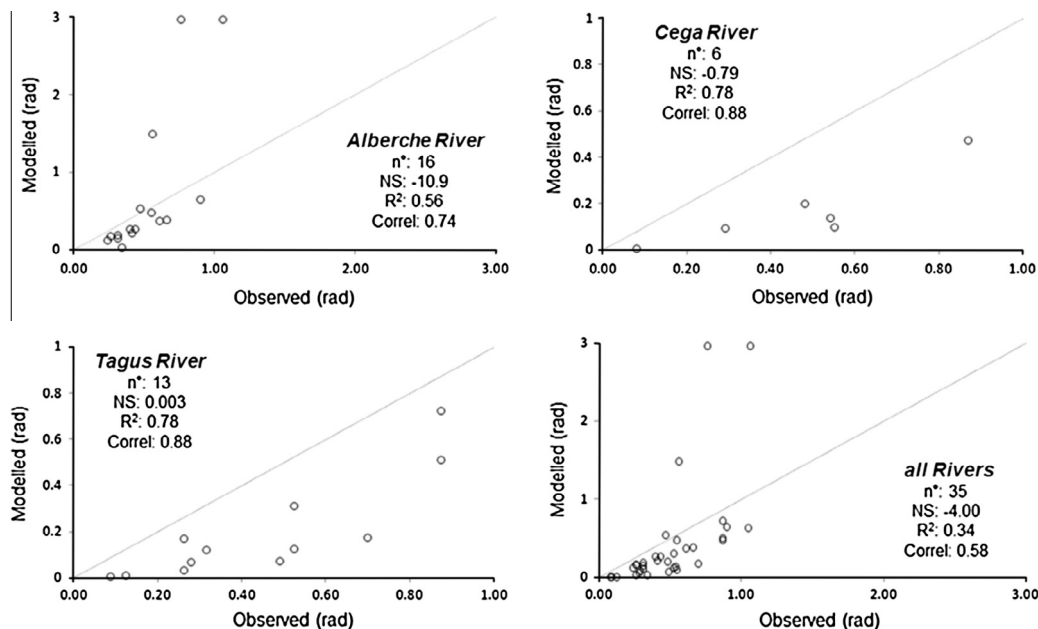


Fig. 4. Comparison between observed and modeled values in the three investigated rivers (Alberche, Cega, Tagus) and in the full dataset.

Table 4

Quantification of uncertainties related to the estimation of model parameters. Parameters are explained in Table 1.

Variable	Units	Values	Uncertainty sources	Changes in results (%)
H_t^*	%	42–15	Epistemic variability derived from the uncertainty (r^2) of the dendrometric models used	112–33
Wood jam	%	±50	Epistemic variability derived from the uncertainty (r^2) of the obtained relations	2
Root-plate size	%	±30	Epistemic variability derived from the uncertainty (r^2) of root-plate models (Ballesteros et al., in preparation)	72
M_{res}	%	±40	Variability inherent to the use of the existing M_{res} model (Stokes, 1999; Bergeron et al., 2009; Nicoll et al., 2008)	29
θ_e	°	5–25°	Variability derived from bibliography, and by varying the elastic angle between 5° and 25°	65

resulted in a change of 21.3%, whereas the same relative change in flow velocities resulted in a variation of results by 24.7%. We also tested the role of M_a , θ_e , D_c and size of the wood deposit volumes. Analysis showed that a variations of these parameters by 20% resulted in comparably smaller changes in the results with 19.1% for θ_e , 17.2% for M_a , 10.4 for D_c and 5% for wood deposit volumes.

4. Discussion

This study relates observed root-plate deformations of riparian trees and results from an empirico-mechanic approach to derive relations between peak discharge in floods and tree tilting in 35 trees in three rivers in Spain. To our knowledge, this is the first attempt to relate tree deformation with the magnitude of past floods, and therefore possibly represents a first step in the direction of introducing a new approach to better appraise and reconstruct paleoflood discharge in ungauged or poorly gauged catchments in the future. Overall, comparison between observed deformations and simulated values points to an underestimation of results by the model. Correspondence between model and field data were much higher in the Tagus and Cega river (NS: ~0), and lower in the Alberche River (NS: -10), where three outliers – i.e. trees tilted during high-magnitude flows – influence the correlation between observations and models. However, despite the complexity of processes involved in flooding in small rivers and the assumptions made during the approach, we realize that moderate to high correlation coefficients exist between observed and modeled values, which clearly points to a relationship between the inclination of trees and flood magnitude.

4.1. Uncertainties and model limitations

Estimation of flood peak discharge, nevertheless, will be subject to several sources of uncertainty (Table 2), mainly related to tree size parameters and the magnitude of the flood itself, and thereby lead to a variability ranging between 33% and 112%. Results also point to the fact that most trees were young and had a small diameter ($DBH = 8.6\text{--}16.6$ cm) when they were tilted. The small size of trees at the time of tilting might have implications on the root-plate system and its capacity to absorb the hydrodynamic forces and tree weight applied to the stem, as some of the energy might have been dissipated in these young trees as a result of elastic deformation of young tree stems. Along these lines of thinking, Neild and Wood (1999) argued that the combined effect of elastic stem models and the root plate could improve the structural modeling of trees against external loads. In view of the discrepancies observed in our data, we speculate that the observed underestimation may be related, among others, to the flow energy dissipated during the elastic deformation of the stem, and thus call for this parameter to be included more explicitly in future modeling approaches.

In this study, the maximum rotational stiffness of the root-plate was assessed a priori and by using a ratio M_{res}/θ_e as suggested in the literature (Coutts, 1983; Blackwell et al., 1990). In addition, we used the approach defined by Peltola (2006) to compute M_{res} as a function of root-plate size. Retrospectively, this assumption may represent the largest source of uncertainty, and further work on this topic might need to reconsider the parameter values chosen. We also linked root-plate sizes with DBH models on the basis of highly resolved GPR imagery and existing models existing in the literature; however, uncertainties quantified from these models may lead to values differing by up to 72% from each other. In addition, the sensitivity analysis suggested that a change of the root-plate size by 20% may lead to variability in results exceeding 50%, so that moderate to high uncertainties have to be expected from this parameter as well.

Another sensitive parameter is elastic limit deformation (θ_e) which average we assessed at 15°, which represents an intermediate value as compared to those reported in literature. For instance, several authors report that the stability of a tree may fail as soon as inclination reaches close to 20° (Cucchi and Bert, 2003; Stokes, 1999), whereas other authors observed that the yield of trees may be associated with rotation values at the base of only 2–5° (Coutts, 1983; Jonsson et al., 2006; Lundström et al., 2007). Very flexible trees have been even reported to return to their upright position after having been deflected to angles >40° (Crook and Ennos, 1998; Ghani et al., 2009). Root deformation was, moreover, found to be about half in young tree trunks and roughly one-third in older trees (Stokes, 1999). Field experiments therefore may improve definition of input data in the model; however, as this value is highly dependent on soil characteristics, tree species, health state and age, high variability can be expected (Crook and Ennos, 1998). We have considered a hypothetical range of values for θ_e between 5° and 20° in this study, which, however, implies changes of up to 65%. In conclusion, our analysis point to the crucial role of M_{res} and θ_e on obtained results, but also indicates that these parameters are the most crucial and difficult to assess, thereby calling for future studies in this direction so as to improve the approach presented here.

Another source of variability is the impact that wood deposits around trees have on tilting. This variable has been included in this paper as an equivalent and punctual force generated by the wooden material as a function of the kinetic energy of the floating wooden mass. Changes of this parameter (20%, sensitivity analysis) did not lead to significant changes in model results. At the same time, however, it is possible that the influence of wood deposits has been underestimated in our approach as we only included them as punctual forces. Under real flood conditions, one might expect that – as a consequence of wood deposit around trees – the surface exposed to the flow will be increased and lead to changes in hydraulic conditions. As a consequence, super-elevations of almost 20 cm may occur upstream of a tree and with a flow velocity <2 m s⁻¹, whereas even larger super-elevations (in the order of 40–80 cm) can be observed as soon as flow velocities are 3–4 m s⁻¹ and based on Bernoulli formula (Borga et al., 2008). This

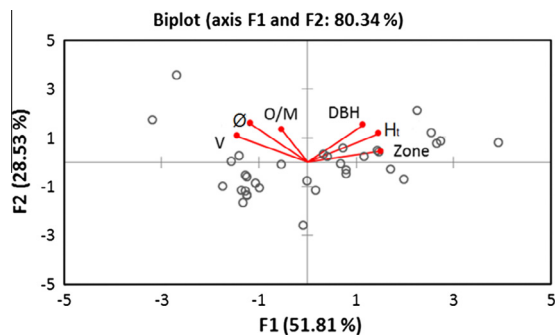


Fig. 5. Principal component analysis (PCA) illustrating two groups of factors explaining most of data variability.

fact may, consequently, explain the existence of three outliers in the Alberche River, even more so as the reconstructed years of tilting match with large floods (i.e. large discharge) and thus higher flow velocities. In addition, based on the inherent complexity and the addition of further uncertainties, we did not consider punctual forces related to other sources of sediment influencing trees, even more so as we assess that the deformation induced by these impacts might be less important in our case as young trees may be in a position to dispel such short charges via the vibration of the tree trunk (Dorren and Berger, 2006).

Another key factor that should be discussed here is related to the influence of trees on flow velocity profiles. The existence of trees significantly modifies the velocity profile in rivers and thereby also the distribution of hydrodynamic pressures on stems (Huai et al., 2009). Changes over water depth can be distinguished especially in case trees are completely submerged which renders flow velocity profiles even more complex (Galema, 2007). In the case of emerged trees, the velocity profile can be fitted with a logarithmic law (Huai et al., 2009). As a consequence, we only used trees whose estimated height (based on the dendrometric model) was greater than the modeled water depth. For this purpose we also checked the expected size of the limit layer at different stem heights using a kinematic viscosity ($15\text{ }^{\circ}\text{C}$) = $1.14\text{E}-06\text{ m}^2\text{ s}^{-1}$ and different water depths (Streeter et al., 2000). The maximum computed value for the limit layer depth for the range of velocities modeled was 5 cm, meaning that the influence of the limit layer on the velocity profile may be neglected in our case. As a further consequence of this finding, we also conclude that flow velocity and water depth modeled with calibrated hydraulics models at the location of trees are indeed valid for the propose of this study.

A drag coefficient value $D_c = 1.00$ has been assumed in this study to estimate the drag force (F_d). However, it has been observed that D_c follows an exponential function which in turn depends on the magnitude of the deformation (Vogel, 1989). Cullen (2005) therefore suggested that D_c on trees may be greater than 1.00 in the case of wind forces. In analogy to Cullen (2005), and with respect to observed flow velocities, D_c may be set at 0.75. In a slightly different context, Bruschi et al. (2003) obtained D_c values ranging from 1.06 to 1.34 for cylinders exposed to water currents with speeds of $0.9\text{--}1.75\text{ m s}^{-1}$. On the other hand, Abbe and Montgomery (1996) state that when considering obstructions formed by woody material, the flow coefficient D_c can be set at about 1.55 but that the allocation should be carefully scrutinized. In view of the sensitivity analysis, varying this coefficient will impact results by 50%. We also observe that a significant exponential reduction of D_c as a consequence of tree deformation during a significant flood event will limit considerably tree resistance capacity to subsequent flows, and thereby restricts the effect of superposition principles, which could thus potentially represent a

large drawback of the approach presented in this study. However, the high correlation coefficients obtained here indicate that the approach is still sensitive to floods and tree size, suggesting that the observed deformation is above all caused by individual extreme events, and not related to an accumulation of several flood events.

Finally, we did not consider effects of time force in deformation. Structural behavior may therefore change according to duration of force application (CTE, 2009). Another enhancement in a possible follow-up study could thus incorporate a multiplication coefficient which takes into account time-force dependence in deformation, as is the case in structural engineering. This means that an analogy could be established between the time of load and the time of flood flows as recorded in hydrographs.

4.2. Implications of the new approach on palaeohydrology

Discharge estimates based on tree tilting holds the potential to become an extremely useful tool for palaeoflood reconstructions, especially in ungauged basin systems. Results can be incorporated in systemic flood-frequency analysis (FFA) in the form of censured data limited by low bounds (Benito and Thorndycraft, 2004; Benito and O'Connor, 2013). In the past, river flows were mostly estimated through the localization and analysis of high-water marks or palaeostage indicators, as well as by applying hydraulic models. Evidence used in reconstructions included geomorphic (i.e. slack water deposits, clay lines, erosion marks; Benito et al., 2003) and botanical features (e.g. lichens, tree scars; Díez-Herrero et al., 2013) as well as documentary sources (writings, drawings, photographs, videos, oral testimonies; Brázdil et al., 2006). Such evidence cannot commonly be found in smaller catchments as typical for uplands, either because the flood regime does not provide the conditions needed for the formation of this evidence, or because it has disappeared or distorted since its formation. Tilted trees have several advantages for a palaeohydrological characterization of past flood events and represent a valuable alternative to conventional sources of palaeostage indicators and consequently river flow data for four main reasons: (i) tilted trees are present in virtually all fluvial systems, from the great rivers of the equatorial and subpolar latitudes, rivers of the temperate and Mediterranean regions, in ephemeral streams of tropical and subtropical areas, and from reaches of the headwaters to river-mouths; (ii) a considerable number of tilted trees can typically be found in a given river reach, which facilitates statistically significant sampling and analysis, and which also helps the calibration and validation of results, as compared to other sources of evidence which are often specific and unique, and difficult to test; (iii) despite existing uncertainties, tilted trees may allow obtaining more hydraulic parameters (i.e., velocity and stream power) than typically obtained with standard methods, for which only depth can be estimated. Therefore, results reconstructed with tilted trees can be correlated much more easily with results obtained with numerical hydrodynamic models and (iv) sites where tilted trees and flow gauges are relatively common can serve the calibration and validation of methods and enables the definition of uncertainty ranges.

Because of the aforementioned advantages, an estimation of flood peak-flows based on tilted trees is thought to be a significant scientific and technical progress in palaeohydrology and should thus be extended to more streams and environments. The approach outlined in this paper may also help the extension of the relationship between basin morphometry and hydrologic response, and this irrespectively of whether they are gauged or not. As a result, the inclusion of tilted trees could help the implementation of holistic methodological approaches for the estimation of discharge quantiles.

5. Conclusion and future outlook

Despite the inherent complexity linked to the structural behavior of trees under flow forces in natural conditions, this study has clearly highlighted a correspondence between tree deflection at the stem base and flood magnitude. This paper also highlighted the main drawbacks and uncertainties related to this approach; it concludes that the most important source of uncertainty is related to the rotational stiffness of the root plate system at the time of tilting. This study clearly highlights the possibilities of using the relationship of discharge and stem tilting as censored data (limited by low bounds) and to include this data on past events in FFA in poorly or completely ungauged basins. To reinforce our hypothesis, we call for future work to focus on the understanding of root-plate stiffness to overturning in riparian systems and waterlogged soil. The development of nonlinear models could be helpful in this respect and should also include soil characteristics or root architecture (Dupuy et al., 2007). Replication of this new proxy is likely to enhance magnitude estimations of past events, in particular also in fluvial environments where other evidence in trees (e.g., scars) is even less frequent. The direct use of the new approach would be related to the understanding of the magnitude of unknown events (St. George, 2010) and its inclusion in hypothetical flood risk analysis.

Acknowledgments

This study has been funded by the research project CGL2010-19274 (projects MAS Dendro-Avenidas) of the Spanish Ministry of Economy and Competitiveness. The authors would like to thank Mario Hernandez and Juan Gabriel Perez for their kind help during fieldwork.

References

- Abbe, T., Montgomery, D., 1996. Large woody debris jams, channel hydraulics and habitat formation in large rivers. *Regul. Rivers Res. Manage.* 12, 201–221.
- Ancelin, P., Courbaud, B., Fourcaud, T., 2004. Development of an individual tree-based mechanical model to predict wind damage within forest stands. *For. Ecol. Manage.* 203, 101–121.
- Arbellay, E., Corona, C., Stoffel, M., Fonti, P., Decaulne, A., 2012. Defining an adequate sample of earlywood vessels for retrospective injury detection in diffuse-porous species. *PLoS ONE* 7, e38824.
- Baker, V., 2008. Paleoflood hydrology: origin, progress, prospects. *Geomorphology* 101, 1–13.
- Baker, V.R., Webb, R.H., House, P.K., 2002. The scientific and societal value of paleoflood hydrology. In: House, P.K., Webb, R.H., Baker, V.R., Levish, D.R. (Eds.), *Ancient Floods, Modern Hazards: Principles and Applications of Paleoflood Hydrology*, Water Science and Application, vol. 5. American Geophysical Union, Washington, DC, pp. 1–19.
- Ballesteros, J.A., Stoffel, M., Bodoque, J.M., Bollschweiler, M., Hitz, O., Díez-Herrero, A., 2010a. Wood anatomy of *Pinus pinaster* Ait. following wounding by flash floods. *Tree Ring Res.* 66 (2), 93–103.
- Ballesteros, J.A., Stoffel, M., Bollschweiler, M., Bodoque, J.M., Díez-Herrero, A., 2010b. Flash-flood impacts cause changes in wood anatomy of *Alnus glutinosa*, *Fraxinus angustifolia* and *Quercus pyrenaica*. *Tree Physiol.* 30, 773–781.
- Ballesteros-Cánovas, J.A., Eguibar, M., Bodoque, J.M., Díez-Herrero, A., Stoffel, M., Gutiérrez-Pérez, I., 2011a. Estimating flash flood discharge in an ungauged mountain catchment with 2D hydraulic models and dendrogeomorphic paleostage indicators. *Hydrol. Process.* 25, 970–979.
- Ballesteros-Cánovas, J.A., Bodoque, J.M., Díez-Herrero, A., Sánchez-Silva, M., Stoffel, M., 2011b. Calibration of floodplain roughness and estimation of palaeoflood discharge based on tree-ring evidence and hydraulic modelling. *J. Hydrol.* 403, 103–115.
- Ballesteros-Cánovas, J.A., Stoffel, M., St George, S., Hirschboeck, K., (in preparation). Flood records in tree rings: a review. *Prog. Phys. Geogr.*
- Benito and O'Connor, 2013. Quantitative paleoflood hydrology. In: Shroder, J.F. (Ed.) *Treatise on Geomorphology*, pp. 459–474.
- Benito, G., Thornycraft, V.R., 2004. Systematic, Paleoflood and Historical Data for the Improvement of Flood Risk Estimation: A Methodological Guide. CSIC, Madrid.
- Benito, G., Thornycraft, V.R., 2005. Palaeoflood hydrology and its role in applied hydrological sciences. *J. Hydrol.* 313, 3–15.
- Benito, G., Sopena, A., Sanchez-Moya, Y., Machado, M.J., Perez-Gonzalez, A., 2003. Palaeoflood record of the Tagus River (Central Spain) during the Late Pleistocene and Holocene. *Quat. Sci. Rev.* 22, 1737–1756.
- Bergeron, C., Ruel, J.-C., Élie, J.-G., Mitchell, S.J., 2009. Root anchorage and stem strength of black spruce (*Picea mariana*) trees in regular and irregular stands. *Forestry* 82 (1), 29–41.
- Blackwell, P.G., Rennolls, K., Coutts, M.P., 1990. A root anchorage model for shallowly rooted Sitka spruce. *Forestry* 63, 73–91.
- Borga, M., Gaume, E., Creutin, J.D., Marchi, L., 2008. Surveying flash floods: gauging the ungauged extremes. *Hydrol. Process.* 22 (18), 3883–3885.
- Braam, R.R., Weiss, E.E.J., Burrough, P.A., 1987. Spatial and temporal analysis of mass movement using dendrochronology. *Catena* 6, 573–584.
- Brázdil, R., Kundzewicz, Z.W., Benito, G., 2006. Historical hydrology for studying flood risk in Europe. *Hydrol. Sci. J.* 51, 739–764.
- Bruschi, G., Nishioka, T., Tsang, K., Wang, R., 2003. A comparison of analytical methods. Drag coefficient of a cylinder. *MAE 171A*. Friday PM3.
- Chiba, Y., 2000. Modelling stem breakage caused by typhoons in plantation *Cryptomeria japonica* forests. *For. Ecol. Manage.* 135, 123–131.
- Chow, V.T., 1959. *Open-channel Hydraulics*. McGraw-Hill, New York.
- Coder, K.D., 2010. *Root Strength & Tree Anchorage*. Warnell School of Forestry & Natural Resources. University of Georgia.
- Coutts, M.P., 1983. Root architecture and tree stability. *Plant Soil* 71, 171–188.
- Crook, M.J., Ennos, A.R., 1998. The increase in anchorage with tree size of the tropical tap rooted tree *Mallotus wrayi*, King (Euphorbiaceae). *Annl. Bot.* 82, 291–296.
- CTE, 2009. Código Técnico de la edificación: Seguridad d estructural madera. Documento básico SE-M. 132.
- Cucchi, V., Bert, D., 2003. Wind-firmness in *Pinus pinaster* Ait. stands in Southwest France: influence of stand density, fertilization and breeding in two experimental stands damaged during the 1999 storm. *Ann. For. Sci.* 60, 209–226.
- Cullen, S., 2005. Trees and wind: a practical consideration of the drag equation velocity exponent for urban tree risk management. *J. Arboric.* 31 (3), 101–113.
- Danjon, F., Fourcaud, T., Bert, D., 2005. Root architecture and wind-firmness of mature *Pinus pinaster*. *New Phytol.* 168, 387–400.
- Díez-Herrero, A., Ballesteros-Cánovas, J.A., Ruiz-Villanueva, V., Bodoque, J.M., 2013. A review of dendrogeomorphological research applied to flood risk analysis in Spain. *Geomorphology* 196, 211–220.
- Dorren, L.K.A., Berger, F., 2006. Stem breakage of trees and energy dissipation during rockfall impacts. *Tree Physiol.* 26 (1), 63–71.
- Dupuy, L., Fourcaud, T., Stokes, A., 2005. A numerical investigation into the influence of soil type and root architecture on tree anchorage. *Plant Soil* 278, 119–134.
- Dupuy, L., Fourcaud, T., Lac, P., Stokes, A., 2007. A generic 3D finite element model of tree anchorage integrating soil mechanics and real root system architecture. *Am. J. Bot.* 94 (9), 1506–1514.
- England, A.H., Baker, C.J., Saunderson, S., 2000. A dynamic analysis of windthrow of trees. *Forestry* 73, 225–237.
- Fourcaud, T., Jin-Nan, J., Zhang, Z., Stokes, A., 2008. Understanding the impact of root morphology on overturning mechanisms: a modelling approach. *Annl. Bot.* 101, 1267–1280.
- Galema, 2007. *Vegetation resistance Evaluation of vegetation resistance descriptors for flood management*. University of Twente.
- Gardiner, B.A., Peltola, H., Kellomäki, S., 2000. Comparison of two models for predicting the critical wind speeds required to damage coniferous trees. *Ecol. Model.* 129, 1–23.
- Ghani, M.A., Stokes, A., Fourcaud, T., 2009. The effect of root architecture and root loss through trenching on the anchorage of tropical urban trees (*Eugenia grandis* Wight). *Trees* 23, 197–209.
- Gottesfeld, A.S., 1996. British Columbia flood scars: maximum flood-stage indicators. *Geomorphology* 14, 319–325.
- House, P.K., Webb, R.H., Baker, V.R., Levish, D. (Eds.), 2002. *Ancient Floods, Modern Hazards: Principles and Applications of Paleoflood Hydrology*. Water Science and Application, vol. 5. American Geophysical Union.
- Huai, W.X., Zeng, Y.H., Xu, Z.G., Yang, Z.H., 2009. Three-layer model for vertical velocity distribution in open channel flow with submerged rigid vegetation. *Adv. Water Resour.* 32, 487–492.
- Husch, B., Miller, C.I., Beerst, T.W., 1982. *Forest Mensuration*. Krieger Publishing Company, Malabar, Florida.
- Jarrett, R.D., 1991. Paleohydrology and its value in analyzing floods and droughts. *US Geol. Surv. Prof. Pap.* 2375, 105–116.
- Jonsson, M.J., Foetzki, A., Kalberer, M., Lundström, T., Ammann, W., Stöckli, V., 2006. Root-soil rotation stiffness of Norway spruce (*Picea abies* (L.) Karst) growing on subalpine forested slopes. *Plant Soil* 285, 267–277.
- Kato, A., Nakatani, H., 2000. An approach for estimating resistance of Japanese cedar to snow accretion damage. *For. Ecol. Manage.* 135, 83–96.
- Lopez-Saez, J., Corona, C., Stoffel, M., Astrade, L., Berger, F., Malet, J.P., 2012. Dendrogeomorphic reconstruction of past landslide reactivation with seasonal precision: the Bois Noir landslide, southeast French Alps. *Landslides* 9, 189–203.
- Lundström, T., Jonsson, M.J., Kalberer, M., 2007. The root-soil system of Norway spruce subjected to turning moment: resistance as a function of rotation. *Plant Soil* 300, 35–49.
- Mikuš, P., Wyzga, B., Kaczka, R.J., Walusiak, E., Zawiejska, J., 2013. Islands in a European mountain river: linkages with large wood deposition, flood flows and plant diversity. *Geomorphology* 202, 115–127.
- Nash, J.E., Sutcliffe, J.V., 1970. River flow forecasting through conceptual models part I – a discussion of principles. *J. Hydrol.* 10 (3), 282–290.

- Neild, S.A., Wood, C.J., 1999. Estimating stem and root anchorage flexibility in trees. *Tree Physiol.* 19, 141–151.
- Nicoll, B.C., Gardiner, B.A., Peace, A.J., 2008. Improvements in anchorage provided by the acclimation of forest trees to wind stress. *Forestry* 81 (3), 389–398.
- Peltola, H.M., 2006. Mechanical stability of tress under static loads. *Am. J. Bot.* 93 (10), 1501–1511.
- Pettit, N.E., Naiman, R.J., Rogers, K.H., Little, J., 2005. Post flooding distribution and characteristics of large woody debris piles along the semi-arid Sabie River, South Africa. *River Res. Appl.* 21, 27–38.
- Ruiz-Villanueva, V., Díez-Herrero, A., Stoffel, M., Bollschweiler, M., Bodoque, J.M., Ballesteros, J.A., 2010. Dendrogeomorphic analysis of flash floods in a small ungauged mountain catchment (Central Spain). *Geomorphology* 118, 383–392.
- Sigafoos, R.S., 1964. Botanical evidence of floods and flood-plain deposition. *US Geol. Surv. Prof. Pap.* 485-A, 1–35.
- St. George, S., 2010. Tree rings as paleoflood and paleostage indicators. In: Stoffel, M., Bollschweiler, M., Butler, D.R., Luckman, B.H. (Eds.), *Tree-Rings and Natural Hazards, A State-of-the-Art*. Springer, New York.
- Stoffel, M., Corona, C., 2014. Dendroecological dating of geomorphic disturbance in trees. *Tree-Ring Res.* 70, 3–20.
- Stoffel, M., Bollschweiler, M., Butler, D.R., Luckman, B.H., 2010. *Tree rings and natural hazards: a state-of-the-art*. Springer, Heidelberg, Berlin, New York.
- Stokes, A., 1999. Strain distribution during anchorage failure of *Pinus pinaster* at different ages and tree growth response to wind-induced root movement. *Plant Soil* 217, 17–27.
- Stokes, A., Salin, F., Kokutse, A.D., Berthier, S., Jeannin, H., Mochan, S., Dorren, L., Kokutse, N., Abd-Ghani, M., Fourcaud, T., 2005. Mechanical resistance of different trees species to rockfall in the French Alps. *Plant Soil* 278, 107–117.
- Streeter, V., Wylie, E., Bedford, K., 2000. *Mecánica de Fluidos*, ninth ed. McGraw Hill.
- Timell, T.E., 1986. *Compression Wood in Gymnosperms*. Springer, Berlin.
- USDA, 1999. *Soil taxonomy. A Basic System of Soil Classification for Making and Interpreting Soil Surveys*. Agriculture Handbook, Number 436. United States Department of Agriculture, Natural Resources Conservation Service, second ed.
- Vogel, S., 1989. Drag and reconfiguration of broad leaves in high winds. *J. Exp. Bot.* 40, 941–948.
- Watson, A., 2000. Wind-induced forces in the near-surface lateral roots of radiata pine. *For. Ecol. Manage.* 135, 133–142.
- Yanosky, T.M., Jarrett, R.D., 2002. Dendrochronologic evidence for the frequency and magnitude of paleofloods. In: House, P.K., Webb, R.H., Baker, V.R., Levisch, D.R. (Eds.), *Ancient Floods, Modern Hazards: Principles and Applications of Paleoflood Hydrology, Water Science and Application*, vol. 5. American Geophysical Union, Washington, pp. 77–89.